Supplementary Information

High Specific Energy Supercapacitor Electrode Prepared from MnS/Ni$_3$S$_2$ Composite Grown on Nickel Foam.

Aya Mohamed[a], N. S.Tantawy[a], S.S. Mahmouad[a], M. A. Shoeib[b] and Saad G. Mohamed[c]*.

[a]Chemistry Department, Faculty of Women for Arts, Science and Education, Ain Shams University, Cairo, Egypt

[b]Department of Surface Technology and Corrosion Protection, Central Metallurgical Researches and Development Institute, CMRDI, P. O. Box: 87, Helwan, Cairo, Egypt

[c]Mining and Metallurgy Engineering Department, Tabbin Institute for Metallurgical Studies (TIMS), Tabbin, Helwan 109, Cairo 11421, Egypt

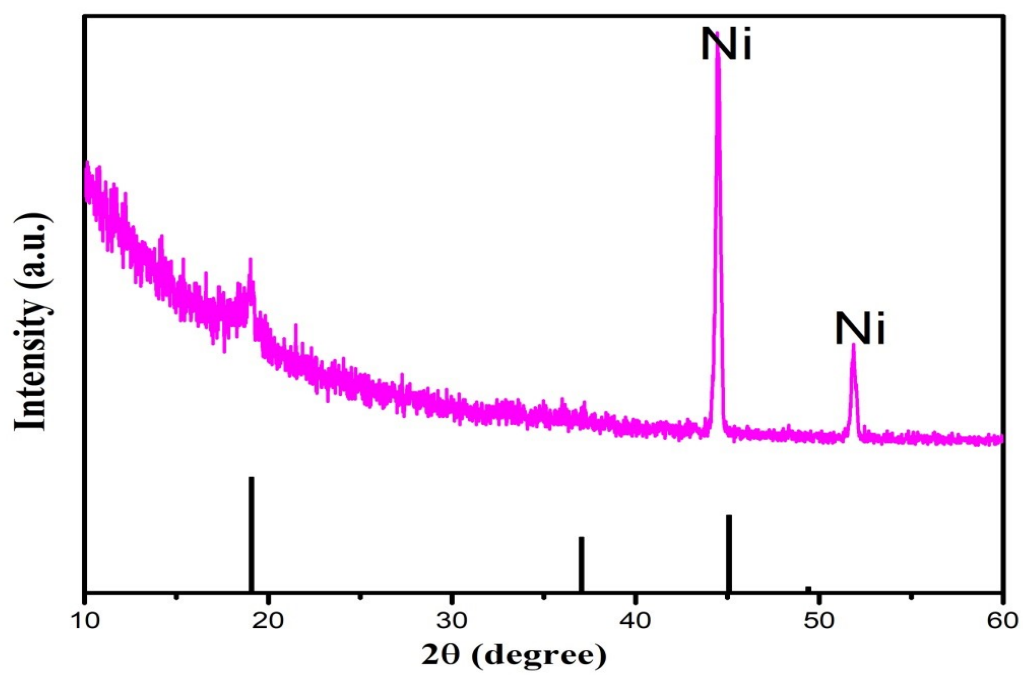*Corresponding author Email address: saadmohamed@tims.gov.eg (S. G. Mohamed)

Fig. S1. XRD pattern of MnO$_2$ on nickel foam reference card [JCPS 42-1169].
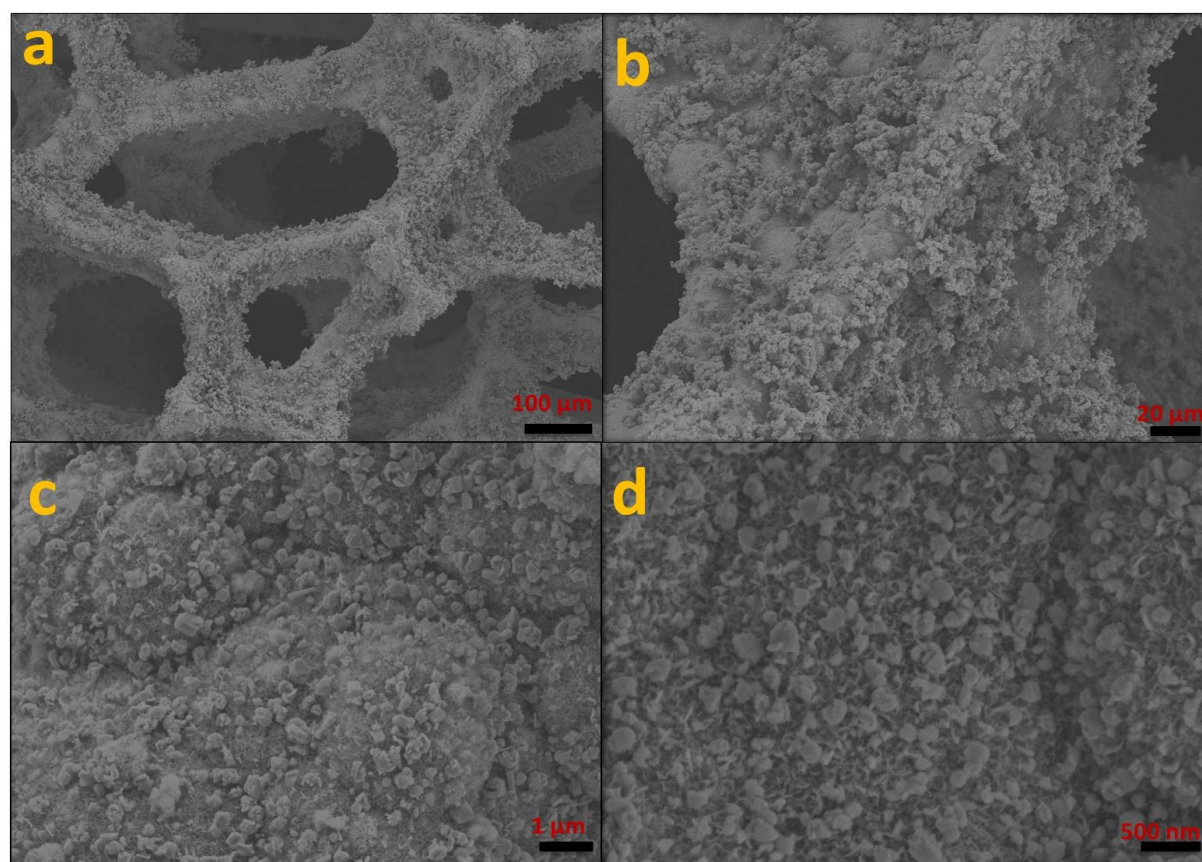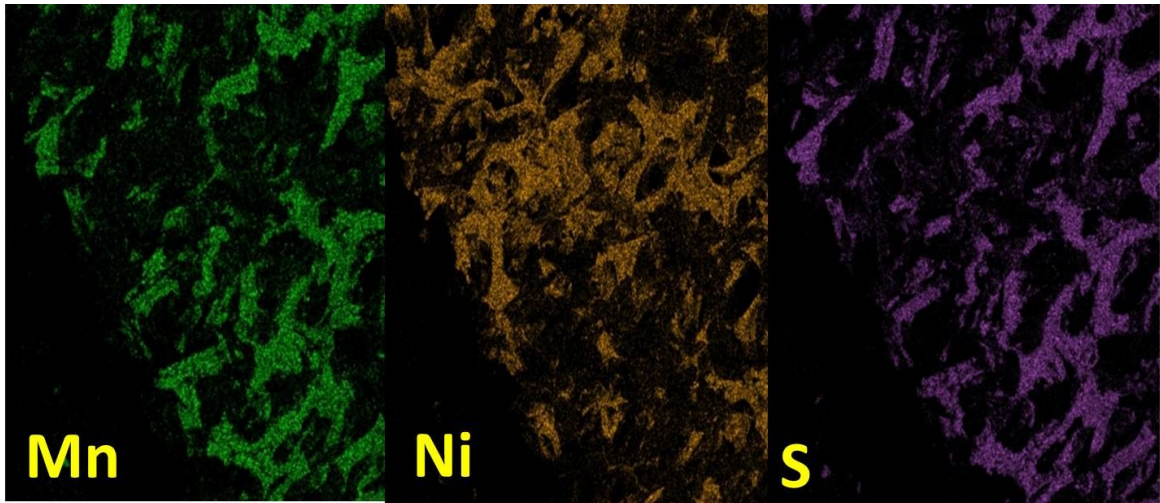

Fig. S2 SEM images of MnO$_2$.

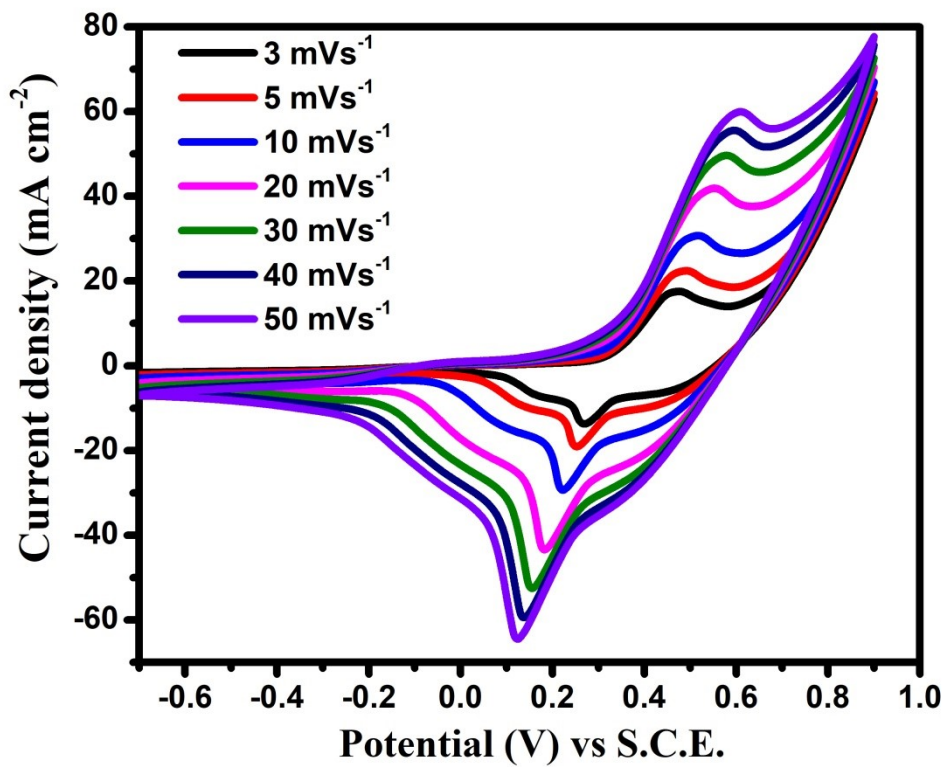Fig. S3 EDX images of MNE electrode.

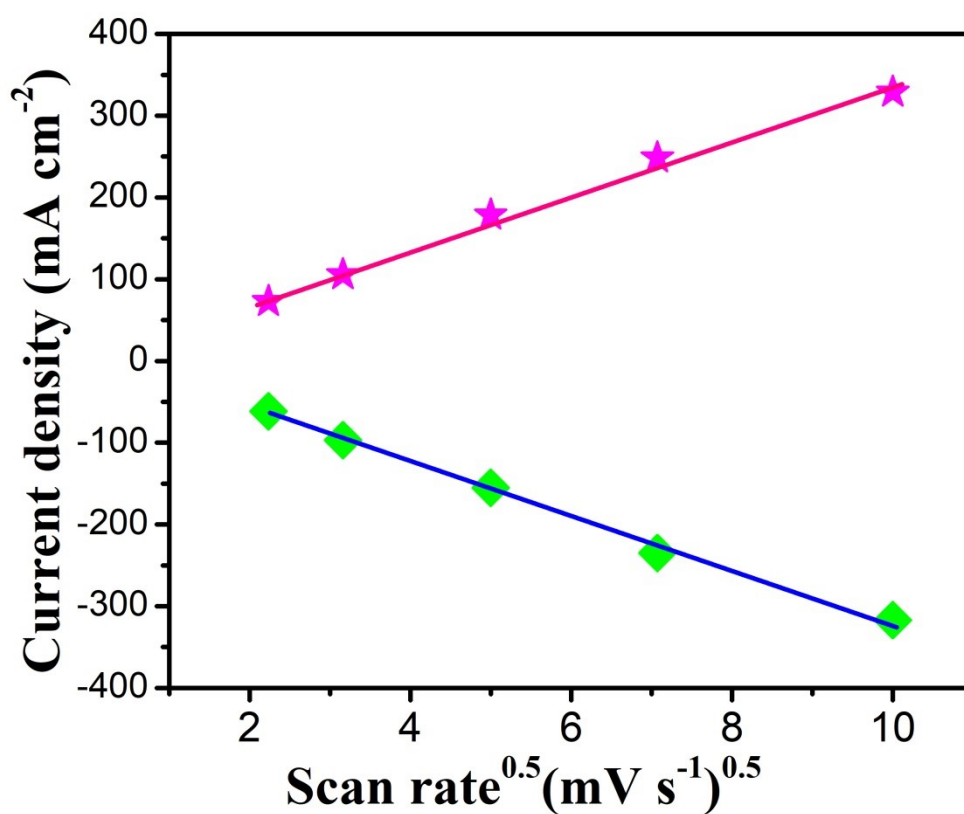Fig. S4 CV curves at different scan rates of MnO_2.

Fig. S5 peak current density as a function of the square root of the scan rate v.

Fig. S6 GCD curves at multiple voltage windows.

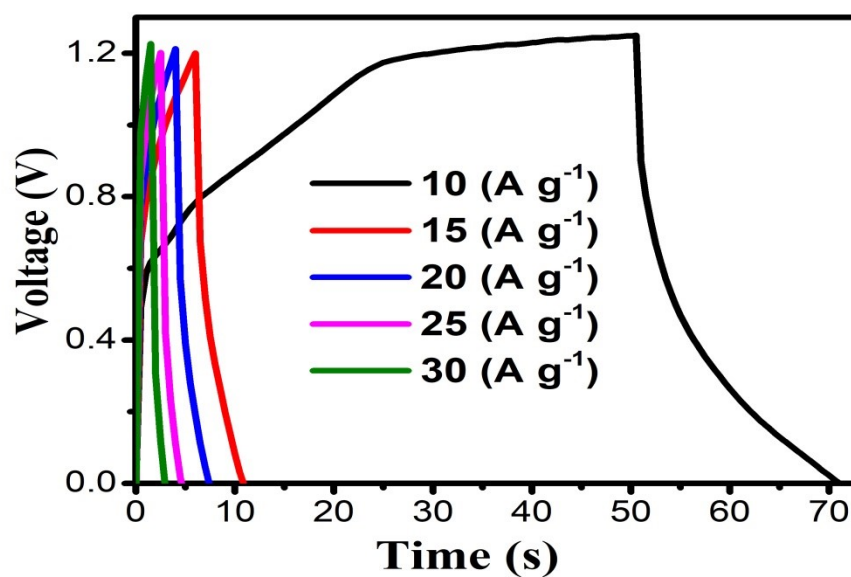Fig. S7 GCD curves at voltage windows1.2 V.

Table S1. Capacity values at different scan rates calculated from CV curves of MNE electrode.

scan rate (mV s^{-1})	capacity (mAh cm^{-2})	surface contribution%	Non-surface contribution%
5	352.5	34.0	66.0
10	294.6	40.7	59.3
25	242.4	49.5	50.5
50	191.1	62.8	37.2
100	126.6	94.8	5.2

Table S2. Areal capacity and capacitance at different current densities calculated from GCD curves of MNE electrode and its comparison with previous works.

Current density	Capacity	Capacitance	reference
3 (mA cm^{-2})	796.7 (mA h cm^{-2})	2390.0 (F cm^{-2})	This work
5 (mA cm^{-2})	651.2 (mA h cm^{-2})	1953.5 (F cm^{-2})	This work
7 (mA cm^{-2})	582.0 (mA h cm^{-2})	1746.0 (F cm^{-2})	This work
10 (mA cm^{-2})	522.7 (mAh cm^{-2})	1568.0 (F cm^{-2})	This work
15 (mA cm^{-2})	454.5 (mA h cm^{-2})	1363.5 (F cm^{-2})	This work
20 (mA cm^{-2})	409.3 (mA h cm^{-2})	1227.8 (F cm^{-2})	This work
25 (mA cm^{-2})	357.3 (mA h cm^{-2})	1071.9 (F cm^{-2})	This work
1 (A g^{-1})	--	1722 (F g^{-1})	Ref.1
2 (A g^{-1})	316.8 (mA h g^{-1})	--	Ref. 2
2 (A g^{-1})	----	373.52 (F g^{-1})	Ref. 3
1 (A g^{-1})	----	547.6 (F g^{-1})	Ref. 4
1 (A g^{-1})	796 (C g^{-1})	2393 (F g^{-1})	Ref..5

Table S3. Specific energy and specific power at different current densities and potential windows, calculated from GCD curves of the hybrid device.

Current density (mA cm^{-2})	Potential window (V)	Time (s)	Specific energy (Wh kg^{-1})	Specific power (W kg^{-1})
30	2	7.0	58.3	30000
35	2	4.7	45.7	35000
40	2	3.8	42.2	40000
45	2	3.0	37.5	45000
50	2	2.4	33.3	50000
25	1.9	8.7	57.4	23750
30	1.9	6.0	47.5	28500
35	1.9	4.3	39.7	33250
20	1.8	15.5	77.5	18000
25	1.8	8.0	50.0	22500
30	1.8	5.5	41.3	27000
35	1.8	3.7	32.4	31500
15	1.6	20.8	69.3	12000
20	1.6	7.7	34.2	16000
25	1.6	5.8	32.2	20000
30	1.6	4.1	27.3	24000
35	1.6	3.2	24.9	28000
5	0.95	14.5	9.6	2375
10	1.2	22.0	36.7	6000
15	1.2	5.8	14.5	9000

20	1.2	4.0	13.3	12000
25	1.2	2.5	10.4	15000
30	1.2	1.5	7.5	18000

References

1 .   Mohamed, S. G.; Hussain, I.; Shim, J.-J. *Nanoscale* **2018**, 10, 6620-6628

2 .   Anil Kumar, Y.; Dasha Kumar, K.; Kim, H.-J. *Dalton Transactions* **2020,** 49, (13), 4050-4059.

3 .   Kumar, M.; Jeong, D. I.; Sarwar, N.; Yoon, D. H. *Ceramics International* **2021,** 47, (12), 16852-16860

4 .   Guanggao, Z.; Menglai, K.; Yadong, Y.; Lu, L.; Minglei, Y.; Xiaoming, L.; Guangfu, Y.; Zhongbing, H.; Abdullah, M. A.; Xuping, S. *Nanotechnology* **2017,** 28, (6), 065402.

5 .   Attia, S. Y.; Barakat, Y. F.; Hassan, H. H.; Mohamed, S. G. *Journal of Energy Storage* **2020,** 29, 101349.